Contents

Introduction

The liquid state of ^{4}He exists in two phases:

- Helium-I: a high temperature phase ($2.17\,\mathrm{K} < T < 4.2\,\mathrm{K}$)
- Helium-II: a low temperature phase ($T < 2.17\,\mathrm{K}$)

These two phases are connected with the *lambda transition*, which occurs at the critical temperature $T_\lambda = 2.17\,\mathrm{K}$ at saturated vapour pressure (**Figure 1**). Helium-I is a classical fluid described by ordinary Navier-Stokes (N-S) equations, whereas Helium-II indicates the Bose-Einstein condensate (superfluid) in much more way.

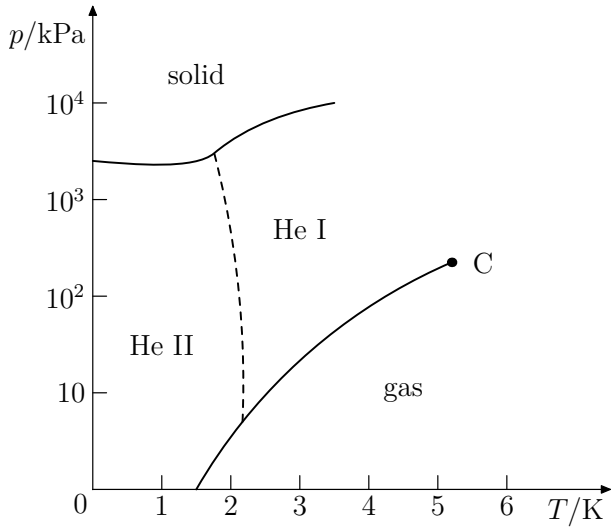

Figure 1: Pressure-Temperature diagram of 4-Helium. Fixing pressure on an atmospheric value, a gas-liquid transition is present at 4.2 K (He-I) and a superfluid transition at 2.17 K.

A simple, phenomenological model of the Helium-II motion was proposed by Tisza [1] and Landau [2] - the *two-fluid model*. According to two-fluid model, it behaves as if composed of two inter-penetrating liquids - the normal and superfluid components - with corresponding velocity fields and temperature-dependent densities:

- normal component: density $\rho_n(T)$, velocity field $\mathbf{v}_n(\mathbf{r}, t)$, motion described by an ordinary viscous Navier-Stokes equation, carrying entropy and thermal excitations represented by *phonons* and *rotons*
- superfluid component: density $\rho_s(T)$, velocity field $\mathbf{v}_s(\mathbf{r}, t)$, motion described by a modified Euler equation (without viscosity) with quantum terms, no entropy, represented by a macroscopic wave function

The total density of Helium-II sums up to $\rho = \rho_n(T) + \rho_s(T) \approx$ const and the relative proportion of normal/superfluid component is determined by the temperature (**Figure 2**). Near $T \to 0$ Helium-II becomes entirely superfluid $\rho_s/\rho \to 1$. The temperature dependence of this ratio is highly nonlinear. For example, the ratio ρ_n/ρ drops from 100% at 2.17 K to 50% at 1.95 K, to $< 5\%$ at 1.3 K, and is effectively negligible under 1 K.

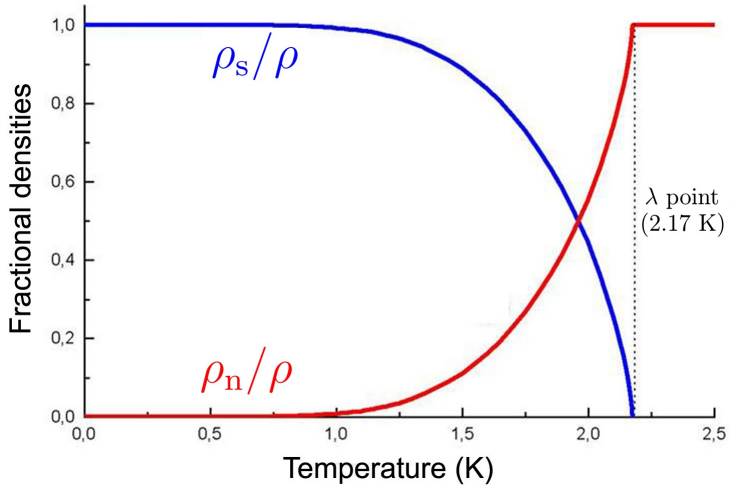

Figure 2: Temperature dependence of fractional densities of the normal (red) and superfluid (blue) components. Source: [3]

While the normal fluid behaves classically, possessing finite viscosity and carrying the entire entropy content of Helium-II, the superfluid component has neither entropy nor viscosity.

It arises from the quantum nature of superfluid, that the superfluid component should not perform any rotation. However, when this component moves faster than a critical velocity, the circulation is *quantized* and so-called *quantized vortices* are created, which makes the hydrodynamics of Helium-II particularly interesting. The vortex nucleation process is still a subject of many current investigations. Superfluid vortex lines can be spatially organized (laminar flows) or completely disorganized (turbulent flows) as simulated in **Figure 3**. Quantum turbulence therefore takes the form of a tangle of quantized vortices in the superfluid component which typically coexist with classical turbulent flow of the normal component.

In the presence of quantized vortices, the independent normal and superfluid velocity fields become coupled by the *mutual friction* force which arises due to quasiparticles scattering off the cores of vortices.

Also we note that below ~ 1 K, a transition to a non-Newtonian ballistic regime occurs in the normal component, similarly as within classical gasses.

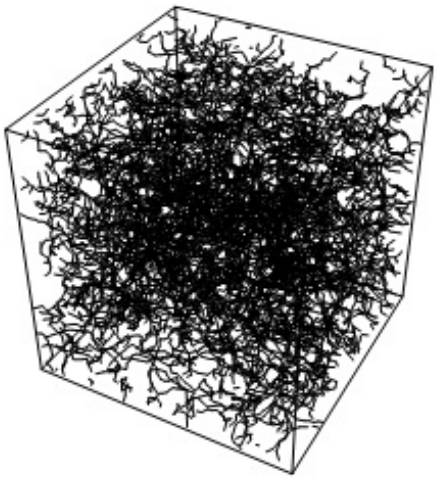

Figure 3: Cube of numerically simulated tangle of randomly distributed quantised vortices. Source: [3]

Quantum turbulence can be experimentally achieved in many traditional ways - driving a mass flow, spinning discs, oscillating grids and forks, ultrasounds and jets.
To characterize the turbulence we use the dimensionless Reynolds number and, recently introduced [4], Donnelly number in their oscillatory form. Examples of already observed quantum flows in He-II were found using oscillatory tools such as grids, tuning forks or discs, were found during experiments in high-frequency regime [5].
We find that for quantum turbulence originated in high-frequency regime above $> 1\,\mathrm{K}$, the emerged drag forces are described in terms of a single dimensionless parameter and exhibit an universal scaling behaviour. We identify and compare the critical conditions related to the production of both quantized vorticity and instabilities occuring in normal component.

Besides experimental approaches on classical fluids, one of the useful tools for understanding the geometry and flow dynamics is the *vortex filament model*, pioneered by Schwarz [6]. With the rapid development of available computational power, large simulations have become the methods of choice for calculating the motion of fluids. In superfluids like Helium-II, due to the quantization of circulation, vorticity can only exist within vortex filaments with a certain core size, which makes the model a way more applicable.
We propose an effective numerical method to compute the time evolution of vortex filaments in superfluid Helium-II. We studied the performance and stability and well replicated the physical processes such as the annihilation of quantized vortex rings [7] while travelling across superfluid.
We also present the `PyVort` code, a new platform in Python 3 to simulate quantum rings phenomena. More on the implementation part can be found in **Simulation** and **Appendix**.

Motivations and Goals

Here we briefly collect all motivations and goals that led us to our investigations.

Experimental approach

- ivestigate transition from classical turbulence to quantum turbulence at various temperatures above $> 1\,\mathrm{K}$ in high-frequency regime.
- construct an experiment using quantum flow generator such as tuning fork and observe the drag phenomena
- apply universal scaling theory and prove the concept on collected experimental data

Simulation

- build modular and reusable codebase in Python 3 with correct physical principles
- implement well stable time-step methods and re-segmentation process
- simulate quantum vortex ring and compare its properties and evolution in time with the theoretical approaches

1. Theoretical Background

The theoretical part of this Thesis is composed of two chapters:

1. Mesoscopic view - provides a theoretical cover of Gross-Pitaevskii theory, creation and numerical modelling of quantum vortex and its dynamics.

3. Macroscopic view - provides a hydrodynamics description of two-fluid model, oscillatory motion in He-II, creation of quantum turbulence, dynamical and universal scaling principles

Aim of the pthepretical art of Thesis is to introduce the basic properties of quantized vortex lines in Helium-II and summarize the state of art of reached knowledge on superfluid turbulence. We also discussed the theoretical methods used to study quantized vorticity, quantum turbulence and the results obtained using such methods.

Micro/Meso-scopic view

One of the most useful ways of describing superfluid helium at $T = 0\,\mathrm{K}$ starts with nonlinear Schrodinger equation (NLSE) for the one-particle wave function ψ. Since the superfluid helium is a strongly correlated system dominated by collective effects, this imperfect Bose-Einstein condensate (BEC) is approximately described by Gross-Pitaevskii equation (1.1). Although, it must be noted that the real Helium-II is a dense fluid, not a weakly interacting Bose gas described by NLSE.

1.1 Gross-Pitaevskii model

In terms of single-particle wavefunction $\psi(\mathbf{r}, t)$ we write the Gross-Pitaevskii model:

$$i\hbar\frac{\partial\psi}{\partial t} = -\frac{\hbar^2}{2m}\nabla^2\psi + \psi\int|\psi(\mathbf{r}', t)|^2 V(|\mathbf{r} - \mathbf{r}'|)\mathrm{d}\mathbf{r}', \tag{1.1}$$

where $V(|\mathbf{r} - \mathbf{r}'|)$ is the potential of two-body interaction between bosons. The normalization is set as $\int|\psi|^2\mathrm{d}\mathbf{r} = N$, where N is number of bosons. By replacing potential with repulsive δ-function of strength V_0 one obtains:

$$i\hbar\frac{\partial\Psi}{\partial t} = -\frac{\hbar^2}{2m}\nabla^2\Psi - m\varepsilon\Psi + V_0|\Psi|^2\Psi, \tag{1.2}$$

where ε is the energy per unit mass and $\Psi = Ae^{i\Phi}$ is a macroscopic wave function of condensate. In this way one can define the condensate's density $\rho_{BEC} = m\Psi\Psi^* = mA^2$ and velocity $\mathbf{v}_{BEC} = (\hbar/m)\nabla\Psi$. Note that equation (1.2) is equivalent to a continuity equation and an modified Euler equation (by the so called quantum pressure term).

Hereafter we identify ρ_{BEC} with helium superfluid component's ρ_s at absolute zero and $\mathbf{v}_{BEC}$ with $\mathbf{v}_s$. It must be noted that this identification is convenient from the point of view of having a simple hydrodynamics model but is not entirely correct. The reason is that Helium-II is a dense fluid, not the weakly interacting Bose gas described by the NLSE (1.1), so the condensate is not the same as the superfluid component.

Even though the superfluid is irrotational: $\omega = \nabla \times \mathbf{v}_s = \mathbf{0}$, the NLSE has a vortex-like solution: $\mathbf{v}_s = \varkappa/2\pi r\, \mathbf{e}_\theta$, where θ is the azimuthal angle and $\varkappa = 9.97 \times 10^{-4}\,\mathrm{cm}^2{\cdot}\mathrm{s}^{-1}$ is the *quantum of circulation*, obtained from:

$$\varkappa = \oint_{\mathcal{C}} \mathbf{v}_{BEC} \cdot \mathrm{d}\boldsymbol{\ell} = \frac{h}{m}\,, \tag{1.3}$$

where $\mathcal{C}$ is a closed loop surrounding the vortex core - a topological defect (**Figure 1.1**) within macroscopic wavefunction Ψ

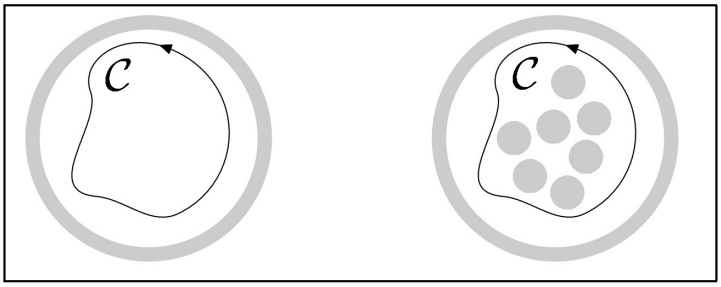

Figure 1.1: An illustration of topological singularities within a classical fluid (on left) and superfluid helium (on right).

1.2 Quantum vortex

As Landau showed [8], superfluid vortex lines appear when Helium-II moves faster than a certain critical velocity. The simplest way to create quantum vortices is to rotate cylinder with superfluid Helium-II with high enough angular velocity Ω. Created vortex lines form an ordered array of density $L = 2\Omega/\varkappa$, all aligned along the axis of rotation (**Figure 1.2**). *Vortex line density* L can be also interpreted as a total vortex length in an unit volume.

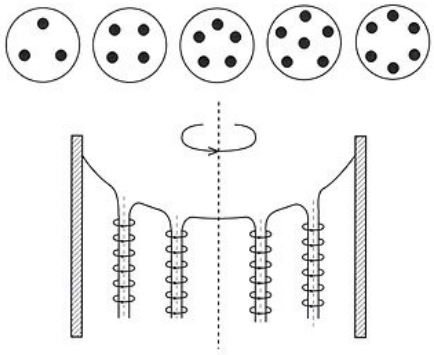

Figure 1.2: Array of quantized vortices in a rotating container

The key properties of Onsager-Feynman vortex [9] are the quantized circulation $\varkappa$, su-

perfluid rotational velocity field $\mathbf{v}_s = \varkappa/2\pi r\,\mathbf{e}_\theta$ and the *vortex core parameter* a_0. The core size a_0 can be estimated by substituting $\mathbf{v}_s$ back into (1.2) and solving differential equation for ρ_s. One finds that ρ_s tends to the value $m^2\varepsilon/V_0$ for $r \to \infty$ and to zero density for $r \to 0$. The characteristic distance over which Ψ collapses (superfluid density ρ_s drops from bulk value to zero) is $a_0 \approx 10^{-10}\,\mathrm{m} = 1\,\text{Å}$. From this, there is a conclusion that the vortex is hollow at its core and therefore, the topological defect occurs.

Taking a_0 as core radius, the energetical calculations showed that N quantum vortices contains more energy than N single quantum vortices. Hence it is generally assumed that only single quantum vortices are commonly observed.

Clearly, vortex lines don't have to be aligned in general. In most cases , the superfluid flow is strongly chaotic, better known as *quantum turbulence*. This topic is covered in more detail later in this work.

1.3 Vortex filament model

The vortex line can be represented as a curve via positional vector $\mathbf{s} = \mathbf{s}(\xi, t)$ in three-dimensional space. Here, ξ is arclength along the vortex line. Next we label $\mathbf{s}'$ as $\mathrm{d}\mathbf{s}/\mathrm{d}\xi$ and $\mathbf{s}''$ as $\mathrm{d}\mathbf{s}'/\mathrm{d}\xi$. Within our context, $\mathbf{s}'$ is a tangent vector and $|\mathbf{s}''|$ is a local curvature R^{-1} at a given point. The triad of vectors $\mathbf{s}'$, $\mathbf{s}''$, $\mathbf{s}' \times \mathbf{s}''$ are perpendicular to each other (**Figure 1.3**) and point along the tangent, normal and binormal respectively:

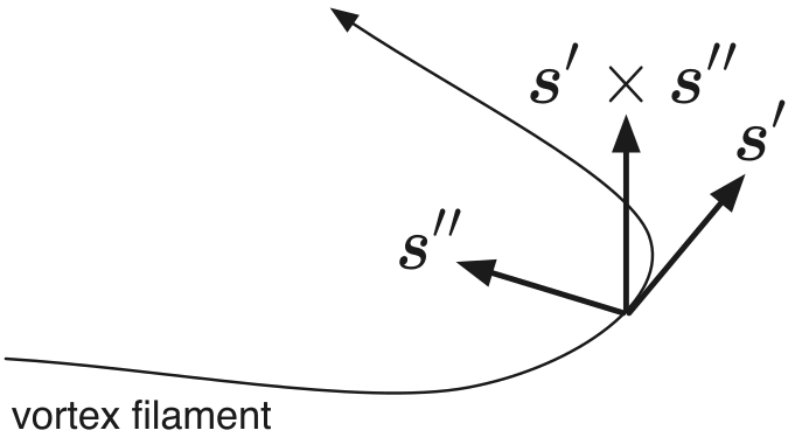

Figure 1.3: Schematic of the vortex filament and the triad vectors $\mathbf{s}'$, $\mathbf{s}''$, $\mathbf{s}' \times \mathbf{s}''$. Source: [**?**]

We suppose that the superfluid component is incompressible $\nabla \cdot \mathbf{v}_s = 0$. Moreover, superfluid vorticity ω_s is localized only at positions of vortex filament $\omega_s(\mathbf{r}, t) = \nabla \times \mathbf{v}_s$. Combining these two properties gives the Poisson equation $\Delta\phi = \omega_s$ for the potential

ϕ. Using Fourier transformation one obtains [10] the Biot-Savart law for the superfluid velocity:

$$\mathbf{v}_s(\mathbf{r}) = \frac{\varkappa}{4\pi} \int_{\mathcal{L}} \frac{(\mathbf{r}' - \mathbf{r}) \times \mathrm{d}\mathbf{r}'}{|\mathbf{r}' - \mathbf{r}|^3}\,, \tag{1.4}$$

where the integral path $\mathcal{L}$ represents curves along all vortex filaments.

This law determines the superfluid velocity field $\mathbf{v}_s(\mathbf{r})$ via the arrangement of the vortex filaments. Now we define the *self-induced* velocity $\mathbf{v}_{\mathrm{ind}}$, describing the motion which a vortex line induces onto itself ($\mathbf{r} \to \mathbf{s}$ in (1.4)) due to its own curvatures:

$$\mathbf{v}_{\mathrm{ind}}(\mathbf{s}) = \frac{\varkappa}{4\pi} \int_{\mathcal{L}} \frac{(\mathbf{r}' - \mathbf{s}) \times \mathrm{d}\mathbf{r}'}{|\mathbf{r}' - \mathbf{s}|^3} \tag{1.5}$$

However, this integral (1.5) diverges as $\mathbf{r}' \to \mathbf{s}$ because the core structure of the quantized vortex was initially neglected. We avoid this divergence by splitting the integral into two parts - direct neighbourhood of the point $\mathbf{s}$ (local part) and the rest $\mathcal{L}'$ (nonlocal part). The Taylor expansion of the local part leads [6] to a finite result:

$$\mathbf{v}_{\mathrm{ind}}(\mathbf{s}) = \mathbf{v}_{\mathrm{ind,local}} + \mathbf{v}_{\mathrm{ind,nonlocal}} \approx \beta \mathbf{s}' \times \mathbf{s}'' + \frac{\varkappa}{4\pi} \int_{\mathcal{L}'} \frac{(\mathbf{r}' - \mathbf{s}) \times \mathrm{d}\mathbf{r}'}{|\mathbf{r}' - \mathbf{s}|^3}\,, \tag{1.6}$$

$$\text{where } \beta = \frac{\varkappa}{4\pi} \ln(R/a_0)\,, \tag{1.7}$$

where $\mathcal{L}'$ is the original vortex line without a close area of the studied vortex point and R is a *local curvature* and often is calculated as $1/|\mathbf{s}''|$ [6].

The local part of induced velocity (1.6) is called as *Local Induction Approximation* (LIA). Since there could be also external flow source of superfluid component, we define the total superfluid velocity, in laboratory frame, as:

$$\mathbf{v}_{s,tot} = \mathbf{v}_{s,ext} + \mathbf{v}_{\mathrm{ind}} \tag{1.8}$$

1.4 Vortex dynamics

To determine the equation of motion of $\mathbf{s}(t)$ we recognize the forces acting upon the line - the magnus force $\mathbf{f}_M$ and (at non-zero temparature $T > 0\,\mathrm{K}$)the drag force $\mathbf{f}_D$ (both are per unit length).

The magnus force $\mathbf{f}_M$ always arises when a rotating body moves in a flow. This emerges a pressure difference, which in our case of moving vortex line with circulation quantum $\varkappa$, exerts a force:

$$\mathbf{f}_M = \rho_s \varkappa \mathbf{s}' \times (\dot{\mathbf{s}} - \mathbf{v}_{s,tot}) \,, \tag{1.9}$$

where $\dot{\mathbf{s}} = \mathrm{d}\mathbf{s}/\mathrm{d}t$ is the velocity of a particular point on a vortex line.

The drag force $\mathbf{f}_D$ arises from the *mutual friction*, the interaction between the normal component and vortex lines (quantized superfluid component). According to the findings of Vinen and Hall [11], the normal fluid flowing with velocity $\mathbf{v}_n$ past a vortex core exerts a frictional force $\mathbf{f}_D$ on the vortex line, given by:

$$\mathbf{f}_D = -\alpha(T)\rho_s \varkappa \mathbf{s}' \times [\mathbf{s}' \times (\mathbf{v}_{ns} - \mathbf{v}_{\mathrm{ind}})] \tag{1.10}$$

$$-\alpha'(T)\rho_s \varkappa \mathbf{s}' \times (\mathbf{v}_{ns} - \mathbf{v}_{\mathrm{ind}}) \,, \tag{1.11}$$

where $\mathbf{v}_{ns} = \mathbf{v}_n - \mathbf{v}_{s,ext}$ is the difference between the average velocity of normal component and the applied superfluid velocity.

The temperature dependent dimensionless parameters $\alpha(T)$ and $\alpha'(T)$ are often written in terms of measured *mutual friction parameters* B and B', which are known from experiments by Samuels and Donnelly [12]:

$$\alpha(T) = \frac{\rho_n B(T)}{2\rho} \qquad \alpha'(T) = \frac{\rho_n B'(T)}{2\rho} \tag{1.12}$$

The precise calculation of the mutual friction parameters $B(T), B'(T)$ over the entire temperature range is still an open problem. Although, we already know that in the area of high temperatures, the friction arises from the scattering processes of rotons.

Since the mass of vortex core is usually neglected, the two forces $\mathbf{f}_M$ and $\mathbf{f}_D$ sum up into zero: $\mathbf{f}_M + \mathbf{f}_D = \mathbf{0}$. Hence, solving for $\mathrm{d}\mathbf{s}/\mathrm{d}t$, we obtain [6] the Schwarz's equation:

$$\dot{s} = \mathbf{v}_{\mathrm{s,\ ext}} + \mathbf{v}_{\mathrm{ind}} + \alpha \mathbf{s}' \times (\mathbf{v}_{ns} - \mathbf{v}_{\mathrm{ind}}) - \alpha' \mathbf{s}' \times [\mathbf{s}' \times (\mathbf{v}_{ns} - \mathbf{v}_{\mathrm{ind}})]\,, \tag{1.13}$$

On the basis of Schwarz's equation (1.13), algorithms to numerically simulate vortex time evolution of an arbitrary configuration can be developed. Also, the vortex parametrisation $\mathbf{s}(\xi, t)$ and dynamics description provide the baseline of what we call as Vortex Filament (VF) model. More on VF model is written later in **Simulation** chapter.

Quantized vortex ring

A special case of vortex line configuration is a freely moving vortex ring. Such rings are usually created as a result of multi-vortex interconnections [7]. The exact expressions derived by classical hydrodynamics [13] for the energy E and induced center velocity v_{ind} of a vortex ring, moving in a Helium-II of density ρ and having a radius R much greater than its core radius $R >> a_0$, are:

$$E = \frac{1}{2}\varkappa^2 \rho R \Big(\ln(8R/a_0) - 2 + c \Big) \tag{1.14}$$

$$v_{\mathrm{ind}} = \frac{\varkappa}{4\pi R} \Big(\ln(8R/a_0) - 1 + c \Big)\,, \tag{1.15}$$

where c is a constant based on inner structure of the vortex. Since we work with hollow core, we use [14] $c = 1/2$. Note that (1.14) and (1.15) depend on a_0 only logarithmically. The behavior of the vortex ring is thus quite insensitive to the exact value of a_0 (expected to be of the order of atomic dimension).

Relations (1.14) and (1.15) are derived directly from hydrodynamical assumptions and no dissipative process (mutual friction) was included. Therefore, the relations hold only for temperature $T = 0\,\mathrm{K}$. The correct form of velocity formula v_{ring} is important to have during simulation for velocity precision tests.

Using explicit dynamical equation [14] for vortex ring motion, one can also derive the final ring center velocity $\mathbf{v}_{\text{ring}}$ and energy E_{ring} using (1.14) and (1.15) like:

$$\mathbf{v}_{\text{ring}} = (1-\alpha')(\mathbf{v}_{\text{ind}} - \mathbf{v}_{\text{s, ext}}) + \alpha'\mathbf{v}_{\text{n, ext}} \tag{1.16}$$

$$E_{\text{ring}} = \Big(\frac{\alpha}{1-\alpha'}\Big)E \tag{1.17}$$

Several other interesting results come from the ring's dynamic motion equation and the mutual friction formula (1.10), (1.11). The second term (1.11) of friction force causes the decrease of vortex ring radius, whereas the first term (1.10) is the dissipative term. The superfluid vortex ring (**Figure (1.4)**) living in a mixture of a normal and superfluid component (temperature $T > 0.6\,\text{K}$) has therefore a limited lifetime expectancy and its travelled distance.

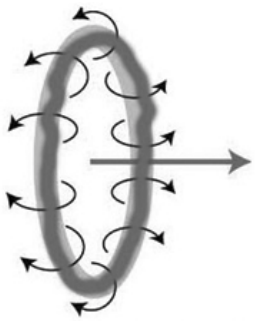

Figure 1.4: Depiction of quantized vortex ring motion and induced velocity field. Source: internet

More explicitly, it was shown [14] that in case of weak counterflow velocity $\mathbf{v}_{\text{ns}}$, the lifetime of vortex ring can be expressed as a simple relation:

$$\tau_{\text{ring}} = \frac{R_0}{2\alpha|\mathbf{v}_i(R_0)|}\,, \tag{1.18}$$

where R_0 is the initial radius of created vortex ring.

By integrating the ring's motion equation from R_0 to $R(\tau) \approx a_0$ we obtain the distance travelled by the ring's center:

$$D_{\text{ring}} = \frac{\alpha}{1-\alpha'}(R_0 - a_0) \tag{1.19}$$

Relations (1.18) and (1.19) are taken as a baseline in **Simulation** chapter.

Macroscopic view

Besides NLSE and Vortex filament model, there is also a third, *macroscopic* model in which the individual vortex lines are *invisible* and Helium-II is considered as a continuous flow of vortices. Many phenomena are similar to those in classical hydrodynamics (**Figure 1.5**), but there emerge also new and very special type of events that can happen within superfluid Helium-II.

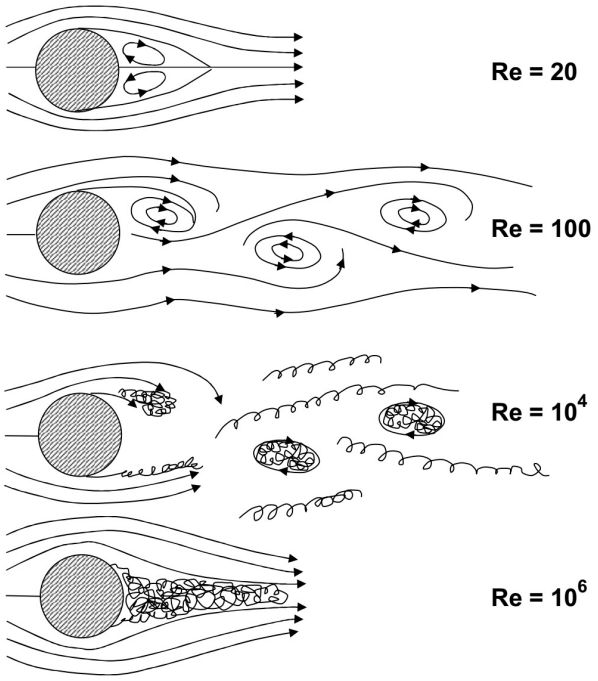

Figure 1.5: Depiction of fluid flow for various Reynolds number values. Many phenomena of laminar, semi-turbulent and turbulent flow are visible in depcitions. Source: [16]

1.5 Hydrodynamics of superfluid

Such macroscopic model is called the HVBK model and provides a generalization of Landau's two-fluid model equations, including the presence of vortices. The superfluid is treated as a continuum and we can define a macroscopic superfluid vorticity $\mathbf{\Omega}_s$, despite the fact that, microscopically, the superfluid velocity field obeys $\nabla \times \mathbf{v}_s = \mathbf{0}$. The downside of this model is its assumption of spatially (not randomly) organized vortices. The common example is a rotating cylinder [15].

The incompressible HVBK equations for normal component $\mathbf{v}_n(\mathbf{r},t)$ and superfluid component $\mathbf{v}_s(\mathbf{r},t)$, respectively, are [10]:

$$\frac{\partial \mathbf{v}_n}{\partial t} + (\mathbf{v}_n \cdot \nabla)\mathbf{v}_n = -\frac{1}{\rho}\nabla P - \frac{\rho_s}{\rho_n} S\nabla T + \frac{\eta}{\rho_n}\nabla^2 \mathbf{v}_n + \mathbf{F}_{ns}\,, \tag{1.20}$$

$$\frac{\partial \mathbf{v}_s}{\partial t} + (\mathbf{v}_s \cdot \nabla)\mathbf{v}_s = -\frac{1}{\rho}\nabla P + S\nabla T + \mathbf{T} - \frac{\rho_n}{\rho}\mathbf{F}_{ns}\,, \tag{1.21}$$

where we have defined:

$$\mathbf{F_{ns}} = \frac{B(T)}{2}\hat{\mathbf{\Omega}} \times [\hat{\mathbf{\Omega}}_s \times (\mathbf{v}_n - \mathbf{v}_s - \nu_s \nabla \times \hat{\mathbf{\Omega}})] + \frac{B'(T)}{2}\mathbf{\Omega}_s \times (\mathbf{v}_n - \mathbf{v}_s - \nu_s \nabla \times \hat{\mathbf{\Omega}}_s)\,, \tag{1.22}$$

$$\mathbf{\Omega}_s = \nabla \times \mathbf{v}_s\,, \tag{1.23}$$

$$\hat{\mathbf{\Omega}}_s = \mathbf{\Omega}_s / |\mathbf{\Omega}_s|\,, \tag{1.24}$$

$$\mathbf{T} = -\frac{\varkappa}{4\pi}\log(b_0/a_0)\mathbf{\Omega}_s \times (\nabla \times \hat{\mathbf{\Omega}}_s) \tag{1.25}$$

Here we can identify the quantities as $\mathbf{F_{ns}}$ (mutual friction force), $\mathbf{T}$ (tension force) and η (viscosity parameter). Usually, b_0 is the intervortex spacing and can be estimated as $b_0 = (2\Omega_s \varkappa)^{-1/2}$. The HVBK equations have reasonably set the limits:

- $T \to T_\lambda$: In this case $\rho_s \to 0$ and the normal fluid motion equation (1.20) becomes the classical Navier-Stokes equation with viscosity term.
- $T \to 0$: In this case $\rho_n \to 0$ and the superfluid motion equation (1.21) describes a pure (potential) superflow. Additionally, taking the classical limit ($\hbar \to 0$) would give us the pure Euler equation of inviscid fluid.

The HVBK model has been widely used with success to study the transition to classical or quantum turbulence, for estimations of critical Reynolds numbers and its temperature dependence.

1.6 Dynamical similarity principle

An important role in behaviour of fluids is taken by the *fluid dimensionless numbers*, which are a set of dynamical quantities representing transport phenomena. In purpose to describe Helium-II with correct equations and with the most precision, we have to choose which dimensionless parameters are useful.

- Knudsen number (Kn): This number helps determine whether statistical mechanics or the continuum mechanics formulation of fluid should be used to model the system. Kn is defined as the ratio of the molecular mean free path length λ (the distance of superfluid atom without excitation) to a representative physical length scale D (container size).
  If temperature of Helium-II rises above $\approx 1.0\,\mathrm{K}$, there is still sufficient amount of normal component and the mean free path of superfluid atoms is much smaller, comparing it with container scale $\lambda \ll D$. In that case, continuum mechanics could be used as a macroscopic theory for superfluid Helium-II.

- Weissenberg number (Wi): This number is used in the study of viscoelasticity of flow. Wi number indicates the degree of anisotropy generated by the deformation, and is appropriate to describe flows with a constant stretch history, such as simple shear. Wi is usually calculated as a multiplication of shear rate $\dot{\gamma}$ and the relaxation time τ.
  Since the relaxation time of Helium-II is relatively small, then $\dot{\gamma}\tau \ll 1$, so the superfluid can be considered as a Newtonian fluid.

- Reynolds number (Re): Let's consider the continuum and newtonian assumptions (Kn $\ll 1$ and Wi $\ll 1$), so the fluid can be described by the raw form of Navier-Stokes (N-S) equation of motion. When we take into account also the incompressibility $\nabla\cdot\mathbf{v} = \mathbf{0}$, the N-S reduces itself to its most simplest form.
  In case of stationary flow ($\partial\mathbf{v}/\partial t = \mathbf{0}$), N-S can be rewritten into a dimensionless form. Following these steps, there arises typical values of velocity U and length scale L, at which there is the most significant change in velocity. Re can be expressed as a ratio of inertial and dissipative forces as $\mathrm{Re} = UL\rho/\eta$, where η is the dynamic viscosity of the flow field.

- Stokes number (St): This number characterizes the bahaviour of particles suspended in a fluid flow. The number is defined as a ratio of characteristic time scale τ of particle and a time scale T of fluid flow, where τ is the relaxation time of particle. If, for a given oscillating body $\tau \gg T$, one may say the body oscillates in the high-frequency regime and particle motion is dominated by its inertia.

The dimensionless scalling of motion equations in fluid mechanics is called as the principle of *dynamical similarity*. Macroscopically it is a phenomenon when comparing two geometrically similar vessels (same shape, different sizes) with the same boundary conditions and the same Reynolds numbers, then the fluid flows will be identical. The derivation of this phenomenon can be directly seen from inspection of the underlying motion equation (1.20), with geometrically similar bodies. In the classical fluid dynamics of ordinary fluids, we use dynamical similarity and scaling arguments for expressing experimental data in terms of Reynolds numbers, drag coefficients, lift, and so on.

Alternatively, the dissipative forces may be described in terms of a dimensionless *drag coefficient* C_D, representing the relation between *drag force* $\mathbf{F}$ and fluid velocity $\mathbf{U}$, and usually takes the form:

$$C_D \propto U^{\alpha}, \qquad \text{where} \begin{cases} \alpha = -1 & \text{for laminar flow } \mathrm{Re} \in (0-10) \\ \alpha = 0 & \text{for turbulent flow } \mathrm{Re} \in (10^3 - 10^5) \end{cases} .$$

It is very common to plot experimentally measured dependence $C_D(\mathrm{Re})$ for various objects (sphere, disc, cylinder) past flow:

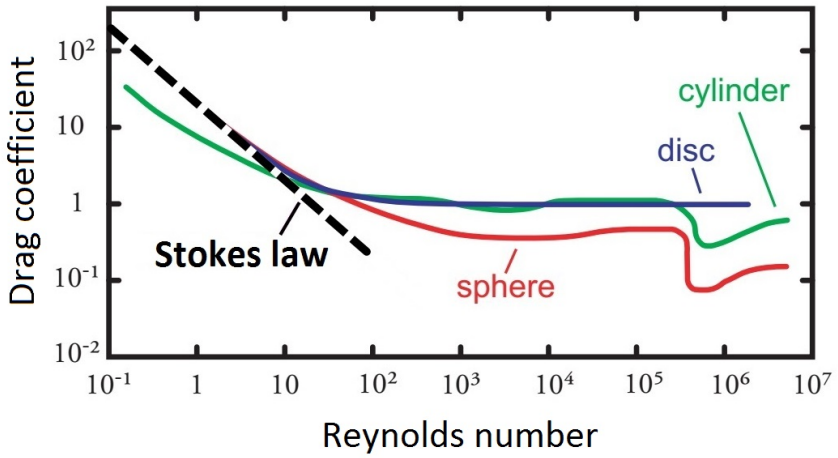

Figure 1.6: Drag coefficients of different objects pas flow with changing Reynlods number. Blue line - thin disc, Green line - cylinder with drag crisis near $\mathrm{Re} \approx 10^6$, Red line - sphere with similar drag crisis as with cylinder, Black dashed line - laminar drag, where $C_D \propto \mathrm{Re}^{-1}$.

Dynamical similarity argument also leads to the existence of critical Reynolds number, at which the transition to turbulence in case of classical fluid occurs. Note that since superfluid Helium-II is composed of two fluids, the mentioned applies only on the normal component. The transition of superfluid component to quantum turbulence is described wider in next chapters

1.7 Oscillatory flows

If a given body is oscillating in a classical viscous fluid, described by ordinary Navier-Stokes equation, the typical length scale L, at which the velocity is changing most significantly, is identified [2] as the *viscous penetration depth*:

$$\delta(\omega) = \sqrt{\frac{2\eta}{\rho\omega}}\,, \tag{1.26}$$

where ω is the angular frequency of oscilations.

Classical hydrodynamics

To describe fully an oscillatory flow, the governing Navier-Stokes equations may be expressed in terms of dimensionless velocity U, time T and positions L. The independent time scale is given by the angular frequency of oscillations ω. Candidates for characteristic lenght scale L may lead to the body size D, surface roughness, or the viscous penetration depth $\delta(\omega)$.

In the high frequency limit $\omega \gg 1$, depending on body geometry, one can reach $\delta(\omega) \ll D$ and say that fluid oscillates in high Stokes regime [4] with $\mathrm{St} = D^2/(\pi\delta^2) \gg 1$. Also, when also the surface roughness exceeds δ, the N-S equation may be expressed using only one dimensionless parameter: an *oscillatory Reynolds number* $\mathrm{Re}_\delta = \delta U\rho/\eta$.

Superfluid Helium-II

Assuming two independent velocity fields $\mathbf{v}_n(\mathbf{r},t)$, $\mathbf{v}_s(\mathbf{r},t)$ in superfluid Helium-II, the above thoughts are applicable for the oscillatory viscous flow of the normal component $\mathbf{v}_n$. We therefore define the high frequency limit for normal component as:

$$\delta_n = \sqrt{\frac{2\eta}{\rho_n\omega}}\,, \qquad \mathrm{D}_n = \frac{U\delta_n\rho_n}{\eta}\,, \tag{1.27}$$

We will call the oscillatory Reynolds number for normal component in superfluid Helium-II as a *Donnelly number* D_n, after Russell J. Donnelly, who as first came with this (1.27) idea.

In low-frequency mode, when $\delta \ll D$ and therefore $\mathrm{St} \gg 1$ (no turbulence produced),

the flow of superfluid component is fully potential, so the normal component will exhibit a laminar viscous flow.

If the typical body curvature is of order $1/D$. the surface may be described as many elements. In this case it is shown [4] that we can write for the average dissipated energy:

$$\langle \dot{E} \rangle = \frac{1}{2} \alpha \xi U_0^2 S_{eff} \sqrt{\frac{\eta \rho_n \omega}{2}} \,, \tag{1.28}$$

where U_0 is the velocity amplitude, S_{eff} the effective surface, α the mutual friction constant and ξ the integral of velocity profile along the resonator. The total energy of an oscillator is given as $E = \xi m U_0^2/2$ and moreover, we define a quality factor Q of an oscillator for an single oscillation as:

$$1/Q = \frac{\langle \dot{E} \rangle}{\omega E} = \frac{\alpha \rho_n S_{eff} \delta_n}{2m} \tag{1.29}$$

From (1.28), one can also derive the peak dissipative in a single oscillation force and the dimensionless drag coefficient related to the normal component:

$$F = \frac{2\omega \langle \dot{E} \rangle}{U_0} = \alpha \xi \omega S_{eff} U_0 \sqrt{\frac{\eta \rho_n \omega}{2}} \quad \rightarrow \quad C_D^n = \frac{2F}{A \rho_n U_0^2} = \frac{2 S_{eff}}{A U_0} \sqrt{\frac{\eta \omega}{\rho_n}} \,, \tag{1.30}$$

where A is the sectional area of the flow. According to dynamical similarity principle, the drag coefficient (1.30) can be expressed as a function of the dimensionless Donnelly number (1.27):

$$C_D^n = \Phi / D_n \,, \tag{1.31}$$

where number Φ is determined by the oscillating body geometry. Clearly, the laminar case of normal component is fully described by the hydrodynamic laws. In turbulent case, we expect a constant value for C_D^n as long, as only normal component contributes to the drag force (no quantum turbulence).

1.8 Quantum turbulence

Turbulence of superfluid component can be viewed as a tangle of vortex lines. In this case quantized vortices can be nucleated either *intrinsically* (such process requires critical velocities of order 10 m/s) or *extrinsically*, by stretching and reconnections of seed vortex loops. The initial vortices in the extrinsical case are the remnant vortices, which always exist in macroscopic samples of Helium-II . In many types of flow the critical velocity for extrinsic vortex nucleation is observed to be in order $\sim$ cm/s.

The superfluid component becomes turbulent at some critical velocity U_C and therefore, we expect an increase in drag coefficient C_D much above the possible dependence caused by turbulence of normal component. The process of self-recconecting remnant vortices was well studied [4] and the related critical velocity is expected to scale as $U_C \propto \sqrt{\varkappa\omega}$. Hence, it is convenient to define a dimensionless velocity $\hat{U}$ with related drag coefficient C_D^s as:

$$\hat{U} = U_0/\sqrt{\varkappa\omega} \quad \rightarrow \quad C_D^s = \frac{2F}{A\rho_s U_0^2} = \frac{2F}{A\rho_s \varkappa\omega \hat{U}^2}\,, \tag{1.32}$$

In case of turbulent superfluid component with velocities sufficiently above critical values, we expect both component to be coupled due to the mutual friction. In this case, both components contribute to the pressure drag, and drag coefficient must be calculated classicaly as $C_D = 2F/(A\rho U^2)$. where ρ is the total density of Helium-II.

Ultra-low temperature regime

In classical fluids, when the mean free path λ of particles becomes comparable to a lenght scale D of the system (Kn ~ 1), the continuum model of the fluid starts to break down and the system cannot be longer described by the Navier-Stokes equations. Similar arguments go when the angular frequency of oscillatory flow ω becomes comparable with the relaxation time τ (Wi $= \omega\tau \sim 1$).
Here, the system ius described as a gas of thermal quasiparticles propagating ballistically through a physical vacuum. Therefore, such system state is called as *balistic regime*.

In practice with superfluid Helium-II, such situation is usually reached by cooling fluid down to ultra-low temperatures. Below $T < 1\,\mathrm{K}$), the normal component is not present anymore, but required cooling to obtain balistic regime (**Figure (1.7)**) is below $T < 0.6\,\mathrm{K}$ (here the Helium-II is better described as a gas than a fluid).

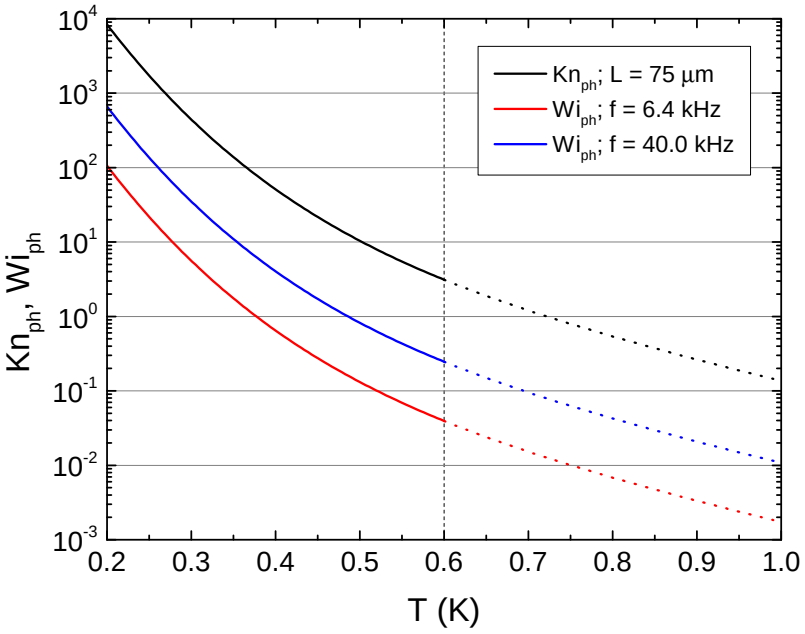

Figure 1.7: Phonon Knudsen number and Weissenberg numbers plotted against temperature for different oscillators. The dashed line separates the interval $T < 0.6\,\mathrm{K}$, where the balistic regime takes a place.

Universal scaling

A study was conducted in order to solve the Stoke's second problem with an oscillating plane in vsicous fluid. This solution is used to derive a universality relation valid in the high frequency limit (with no turbulence present) across both Newtonian and non-Newtonian regimes of the fluid. Using scaling function $f(\omega\tau)$, the authors derived the relation for the quality factor:

$$1/Q = \frac{\alpha S_{eff}}{m}\sqrt{(\frac{\eta\rho_n}{2\omega})}f(\mathrm{Wi}) \tag{1.33}$$

In **Results** we use this form of universality scaling for comparison against experimental data collected in temperature ranges $T < 0.6\,\mathrm{K}$ or $T > 1\,\mathrm{K}$.

Multiple critical velocites

Here is briefly commented the transition to quantum turbulence regime observed at very low temperatures ($T \ll 1\,\mathrm{K}$). A couple of experimental studies in milliKelvin temperatures reported [17] the existence of more critical velocities related with superfluid component flow within single experiment:

- First critical velocity is related with the formation of quantum vortex rings near the surface of oscillating body - possibly forming a thin layer of different hydrodynamic behaviour. Such critical velocity is hard to observe at higher than ultra-low temperature.

- Second critical velocity is a consequence of escaping vortex rings from the oscillator body and forming a superfluid bulk or, eventually, the whole turbulent tangle. Here the sudden raise of drag is observed, usually with hysteresis effect.

- Third critical velocity is the highest critical velocity, which can be observed. The origin of this velocity is hidden in the development of larger quantized vortex structures, which in larger scale become to mimic the classical turbulence. Such velocity is in order $\approx$ m/s and moreover, very likely screened by the influence of the normal component turbulence. Therefore, not likely reachable within experiments reported in this thesis.

Bibliography

[1] Tisza, L. *The viscosity of liquid helium and the Bose-Einstein statistics.* Comptes Rendus Acad. Sciences, **207**:1186-1189 (1952)

[2] Landau, L.D. and Lifshitz, E.M. *Fluid Mechanics*, Second English Edition. Pergamon Books Ltd., (1987). ISBN 0-08-033933-6

[3] Bahyl, J. *Measurement of quantum turbulence in superfluid He-4.* Student conference, FMPH UK, Bratislava (2016)

[4] Jackson, M.J., Schmoranzer, D., et al. *Universal Drag Force Scaling in High Stokes Number Oscillatory Flows of He II.* Phys Rev B, **submitted** (2018)

[5] Schmoranzer, D., Jackson M.J., et al. Phys Rev B, **94** (2016)

[6] Schwarz, K.W. *Three-dimensional vortex dynamics in superfuid He 4: Homogeneous superfluid turbulence*
Phys Rev B, Vol. **38**, 4 (1988)

[7] Rayfield, G.W., Reif F. *Quantized Vortex Rings in Superfluid Helium* Phys. Rev. A, **136**, 5A (1964)

[8] Landau, L.D. *The theory of superfluidity of helium II*
J. Phys. USSR, Vol. **11**, 91 (1947)

[9] Feynman, R. *Application of quantum mechanics to liquid helium.*
Progress in Low Temp Phys, **1**, 17-53 (1957)

[10] Baggaley, A.W. *Superfluid vortices and Turbulence.* Quantized Vortex Dynamics and Superfluid Turbulence, Chap.1, Barenghi C.F. (2001)

[11] Vinen, W.F. and Hall, H.E. *The theory of mutual friction in uniformly rotating helium II.* Proc. Royal Soc. London 238 (1957) 204

[12] Donnelly, R.J., Barenghi, C.F *The Observed Properties of Liquid Helium at the Saturated Vapor Pressure.* American Ins. of Phys. and Chem. Soc. (1998)

[13] Roberts, P.H. Phys. Rev. A, 55, 1971

[14] Donnelly, R.J. *Quantized Vortices in Helium II.*
Cambridge studies in low temp. phys. (2005)

[15] Osborne, D.V. *The Rotation of Liquid Helium-II.*
Proc. Royal Soc. London , **63**: 909-912 (1950)

[16] Van Dyke, M. *An Album of Fluid Motion.*
The Parabolic Press, Stanford, California (1982). ISBN 0-915760-02-9

[17] Nichol, H.A., Skrbek, L. et al. Phys. Rev. Lett. **92**, (2004).

[18] Tsubota, M., Fujimoto, K., Yui S. *Numerical Studies of Quantum Turbulence.*
Journal of Low Temp Phys, 188 (2017)

[19] Baggaley, A.W., Barenghi, C.F. *Tree Method for Quantum Vortex Dynamics.*
Journal of Low Temp Phys, 166 (2012)

[20] Barnes, J., Hut, P. *A hierarchical O(N log N) force-calculation algorithm.* Nature, **324**, 446 (1986)